Drug-induced cellular death dynamics monitored by a highly sensitive organic electrochemical system

Biosensors and Bioelectronics 68 (2015) 791–797

Contents lists available at ScienceDirect

Biosensors and Bioelectronics

journal homepage: www.elsevier.com/locate/bios

Drug-induced cellular death dynamics monitored by a highly sensitive organic electrochemical system

Agostino Romeo [a,1], Giuseppe Tarabella [a,1], Pasquale D'Angelo [a,*], Cristina Caffarra [b], Daniele Cretella [b], Roberta Alfieri [b], Pier Giorgio Petronini [b], Salvatore Iannotta [a,*]

[a] Institute of Materials for Electronics and Magnetism, National Research Council, Parco Area delle Scienze 37/A, Parma 43124, Italy
[b] Unit of Experimental Oncology, Department of Clinical and Experimental Medicine, University of Parma, Parma 43125, Italy

ARTICLE INFO

Article history:
Received 11 November 2014
Received in revised form
22 January 2015
Accepted 31 January 2015
Available online 7 February 2015

Keywords:
Biosensing
Cell death dynamics
Organic Electrochemical Transistor
Apoptosis/necrosis
Pharmacokinetics

ABSTRACT

We propose and demonstrate a sensitive diagnostic device based on an Organic Electrochemical Transistor (OECT) for direct in-vitro monitoring cell death. The system efficiently monitors cell death dynamics, being able to detect signals related to specific death mechanisms, namely necrosis or early/late apoptosis, demonstrating a reproducible correlation between the OECT electrical response and the trends of standard cell death assays. The innovative design of the Twell-OECT system has been modeled to better correlate electrical signals with cell death dynamics. To qualify the device, we used a human lung adenocarcinoma cell line (A549) that was cultivated on the micro-porous membrane of a Transwell (Twell) support, and exposed to the anticancer drug doxorubicin. Time-dependent and dose-dependent dynamics of A549 cells exposed to doxorubicin are evaluated by monitoring cell death upon exposure to a range of doses and times that fully covers the protocols used in cancer treatment. The demonstrated ability to directly monitor cell stress and death dynamics upon drug exposure using simple electronic devices and, possibly, achieving selectivity to different cell dynamics is of great interest for several application fields, including toxicology, pharmacology, and therapeutics.

1. Introduction

Monitoring cell stress and death induced by drug treatments is an issue of great relevance, in particular impacting on toxicology, pharmacology, and therapeutics (Hotchkiss et al., 2009). Cell death is typically discussed dichotomously as either apoptosis or necrosis, although other death mechanisms have been identified so far (Kroemer et al., 2009). Cell death represents sometimes a pathological event or a physiological process: this non-trivial cause–effect correlation makes cell death detection a critical diagnostic issue. A wide number of methods are used for cell viability detection (Stoddart, 2011), providing high throughput results, together with reliability and sensitivity. Nevertheless, they often require expensive laboratory equipments or biological kits, as well as specialized expertize and, in general, do not give real time monitoring. This has generated an increasing demand for easier, faster and portable tools for cell viability screening. Even towards a perspective of a point-of-care approach, easy-to-use, real-time, and reliable devices for the detection and monitoring of processes and dynamics deriving from the drug-cell interaction would be very relevant for modern healthcare. Indeed, the development of such rapid, user-friendly and cost-effective technologies would improve drug-screening protocols and could open new perspectives in therapeutics and theragnostic approaches.

Organic and flexible electronics, because of the unique ability of some π-conjugated polymers to conduct both electronic and ionic carriers (Tarabella et al., 2013a), has been gaining an increasingly relevant role in interfacing sensors with biological systems (Berggren and Richter-Dahlfors, 2007; Cicoira and Santato, 2013; Iannotta et al., 2015; Rivnay et al., 2014). In particular, Organic Electrochemical Transistors (OECTs) are a class of organic-based devices, where the active material forming the transistor channel is made of a conducting polymer, the most popular being the biocompatible *p-type* poly(3,4-ethylenedioxythiophene):polystyrene sulfonate (PEDOT:PSS) (Zhu et al., 2004). In OECTs the conducting polymer is separated from the gate electrode by means of an ionically conducting, electronically dielectric electrolyte. The working principle of an OECT (usually operated in depletion-mode) is based on the modulation of the drain-source current (I_{ds}) flowing through the conducting polymer channel induced by applying a positive gate voltage (V_{gs}). Cations from the electrolyte penetrate the PEDOT:PSS channel upon gate biasing and compensate the doping of the polymer, decreasing its conductivity

* Corresponding authors.
E-mail addresses: pasquale.dangelo@imem.cnr.it (P. D'Angelo), iannotta@imem.cnr.it (S. Iannotta).
[1] Contributed equally to this work.

http://dx.doi.org/10.1016/j.bios.2015.01.073
0956-5663/

(Bernards and Malliaras, 2007; Tarabella et al., 2010). Key features of OECTs are as follows: operation in aqueous environment, low operating voltages and excellent direct amplified ionic-to-electronic signals transduction. These features make OECTs particularly well suited for interfacing and studying cells. In fact, biological applications of OECTs have been recently proposed, dealing with: delivering neurotransmitters in vivo (Simon et al., 2009), electronically controlling ion signaling (Isaksson et al., 2007), controlling cell adhesion (Bolin et al., 2009; Wan et al., 2009) and migration (Gumus et al., 2010), measuring neuronal activity in vivo (Khodagholy et al., 2013), sensing of biomolecules (Kergoat et al., 2014; Lin et al., 2011; Tarabella et al., 2013b, 2012), and fabricating ion-based logic circuits (Tybrandt et al., 2012). Various examples of organic devices interfacing layers of mammalian cells have been recently described too, with applications in toxicology and diagnostic monitoring (Jimison et al., 2012; Lin et al., 2010; Ramuz et al., 2014; Tria et al., 2014; Yao et al., 2013).

In particular, Jimison et al. (2012) have proposed an OECT operating with a Transwell (Twell) micro-porous membrane to study the integrity of a gastrointestinal barrier tissue formed by Caco-2 cells on the Twell. They also demonstrated the ability of effectively monitoring the integrity of such barrier tissue by analyzing the ion transport across tight junctions (multi-protein complexes that form a seal between adjacent cells) upon exposure to chemicals (Jimison et al., 2012; Tria et al., 2013) or bacteria (Tria et al., 2014). In their system the gate electrode was immersed into the electrolyte above the barrier tissue, which, when tight junctions are formed, inhibits the migration of ions towards the OECT polymer channel. Their sensing device is suitable for high throughput in-vitro toxicology applied to detect minute disruptions of the barrier tissue. We were inspired by this work, and challenged by the idea to study viability of cells not necessarily forming barrier tissues. In this case, when a tight junction is not formed, the major issue to face concerns the presence of a large flux of background ions when the gate is turned on, which would make practically impossible to sensitively monitor effects on viability of cells. We hence designed a combined system (hereafter referred to as a Twell-OECT) where the electric force induced by the gate electrode would not directly act on the ions in the electrolyte above, but on a water buffer layer, positioned underneath between the Twell and the PEDOT:PSS film. Therefore the gate voltage would strongly push only the ions after they cross the Twell membrane, the amount of which would depend mainly from the viability of the cells adherent to the Twell membrane. Another possible solution would have been growing directly the cells onto the PEDOT:PSS channel, but, unfortunately, as our experiments confirm, PEDOT:PSS properties are affected by exposure to an electrolyte with high ionic density and rich of a variety of complex species, as in the case of culture growth media.

In this work, by developing this novel Twell-OECT architecture, we aim at demonstrating a sensitive and disposable organic-based sensor for in-vitro monitoring of cellular dynamics, including stress and death. In particular, we studied the viability of a human Non-Small-Cell-Lung-Cancer (NSCLC) cell line (A549), cultured on the Twell that are known not to form tight junctions (Carterson et al., 2005; Heijink et al., 2010). Cell viability was investigated upon exposure to doxorubicin, one of the most frequently used DNA-damaging drugs in cancer chemotherapy (Yang et al., 2014). In order to reliably correlate the device response to changes in cell viability, the time-evolution of cell death was studied upon exposure of cells to series of selected doses of doxorubicin, and for three different exposure times. Results were interpreted by modeling the Twell-OECT device and validated by correlating the device response with traditional methods for cell viability/death assessment. We believe that our technique represents a viable and useful tool complementary to classical cell viability/death assays, since ideally suitable for direct monitoring and real-time screening of drug action.

2. Materials and methods

2.1. OECT fabrication

For the fabrication of OECT devices a standard protocol was used (DeFranco et al., 2006). Transistor channels, made of PEDOT:PSS, were patterned on glass slides using standard photolithographic techniques. PEDOT:PSS was supplemented with ethylene glycol 20% and DBSA 5% in order to improve its conductivity and film formation properties, respectively, and then spin-coated on the glass substrate at 1500 rpm for 30 s. Subsequently to spin-coating, devices were baked for 1 h at 120 °C. The resulting transistor channel was 1 mm wide and ~100 nm thick. Wells for the lodgment of Twell were made of Sylgard 184, poly(dimethylsiloxane) (PDMS) mixed with a curing agent (volume ratio 10:1) and designed with internal volume of ~200 μL. The mixture was cured for 1 h in an oven at 60 °C.

2.2. OECT measurements

Throughout this work, OECT electrical measurements were performed using two Keithley 2400 SourceMeters, controlled by a home-made LabView software, and an Ag wire was used as gate electrode. All measurements were carried out inside a cell-incubator in a water-saturated atmosphere of 5% CO_2 in air at 37 °C, and performed in three replicates for each drug condition. Standard deviations were used for error bars.

2.3. Cell culture

Human non-small-cell lung carcinoma cell line A549, purchased from ATCC (Manassas, VA, USA), was cultured in Petri dishes using RMPI-1640 containing 10% FBS (Gibco, Life Technologies), 1% penicillin/streptomycin solution (Sigma Aldrich) and 2 mM glutamine (Sigma Aldrich). Cells were maintained under standard cell culture conditions at 37 °C in a water-saturated atmosphere of 5% CO_2 in air. For all experiments, A549 cells were seeded in Twells supports (0.4-μm pore size and membrane area of 0.33 cm^2) at the density of 1×10^5 cells/insert, and left to grow reproducibly in a monolayer for 48 h prior to any electrical measurement.

2.4. Drug treatment

Stock doxorubicin (Sigma Aldrich) solutions were prepared using dymethilsulfoxide (DMSO, Sigma Aldrich) as solvent, and diluted in fresh medium before use. Final DMSO concentration in medium never exceeded 0.1% (v/v) and equal amounts of the solvent were added to control cells.

2.5. Cell death quantification

Cell death was also assessed using fluorescence microscopy as complementary technique to the electrical one. A549 cells were cultivated on standard 96-wells plates at the same seeding densities used in Twell supports, and stained with the fluorescent DNA-binding dyes Hoechst 33342 (3 μg/ml) and Propidium Iodide (2.5 μg/ml). The nuclear morphology of control and doxorubicin-treated A549 cells was examined by means of fluorescence and bright field microscopy, as previously described (Cavazzoni et al., 2008).

Cell viability was also assessed by tetrazolium dye [3-(4,5-dimethylthiazol-2-yl)-2,5-diphenyltetrazolium bromide (MTT),

Sigma, Dorset, UK] assay as previously described (Cavazzoni et al., 2008). 3×10^3 cells (A549 cell line) were seeded into 96-wells plates in quadruplicate and treated with increasing concentrations of doxorubicin. After 72 h exposure, cell viability was evaluated by addition of the MTT solution (1 mg/ml). After 2 h of further incubation the formed formazan dye was dissolved using dimethyl sulfoxide (DMSO) and quantified via spectrophotometry. Data are expressed as percent inhibition of cell viability versus control cells.

3. Results and discussion

3.1. Working principle and characterization of the device

Our Twell-OECT architecture is based on the idea of separating the ion detection from the ion drifting mechanisms. We therefore introduced a thin layer of pure water between the Twell and the OECT where the gate electrode operates. In this way the driving force, pushing the ions through the pores of the Twell membrane, is the gradient of concentration, it is practically not affected by the gate voltage, and, hence, becomes dependent only on the surface of open pores as described in detail in the following. Fig. 1a shows the schematic view of the experimental setup, where the Twell is integrated with the OECT by means of a dedicated reservoir made of poly(dimethylsiloxane) (PDMS). The PDMS reservoir is designed with a 1 mm high step at its base, so that the Twell can be reproducibly and precisely positioned, avoiding any potential damage of the transistor channel. Bi-distilled water is used to fill the small gap between the PEDOT:PSS film and the bottom part of the Twell. The area of the polymer in contact with the water defines the active transistor channel. Cell culture medium is confined in the Twell so that the underneath water layer is not exposed to it when the membrane pores are occluded. The water, in contact with PEDOT:PSS, plays the role of an electrolyte at *zero ionic* concentration that, when inseminated by ions coming from the overlying culture medium, flowing through the Twell membrane, makes the OECT sensitive to very small changes in ion concentration. A gate electrode (consisting of a silver wire) is immersed in the bi-distilled water layer, i.e. *not directly in contact with the culture medium*, hence achieving the goal of separating detection from ion drifting mechanisms. This configuration also strongly reduces the mentioned deterioration of the PEDOT:PSS

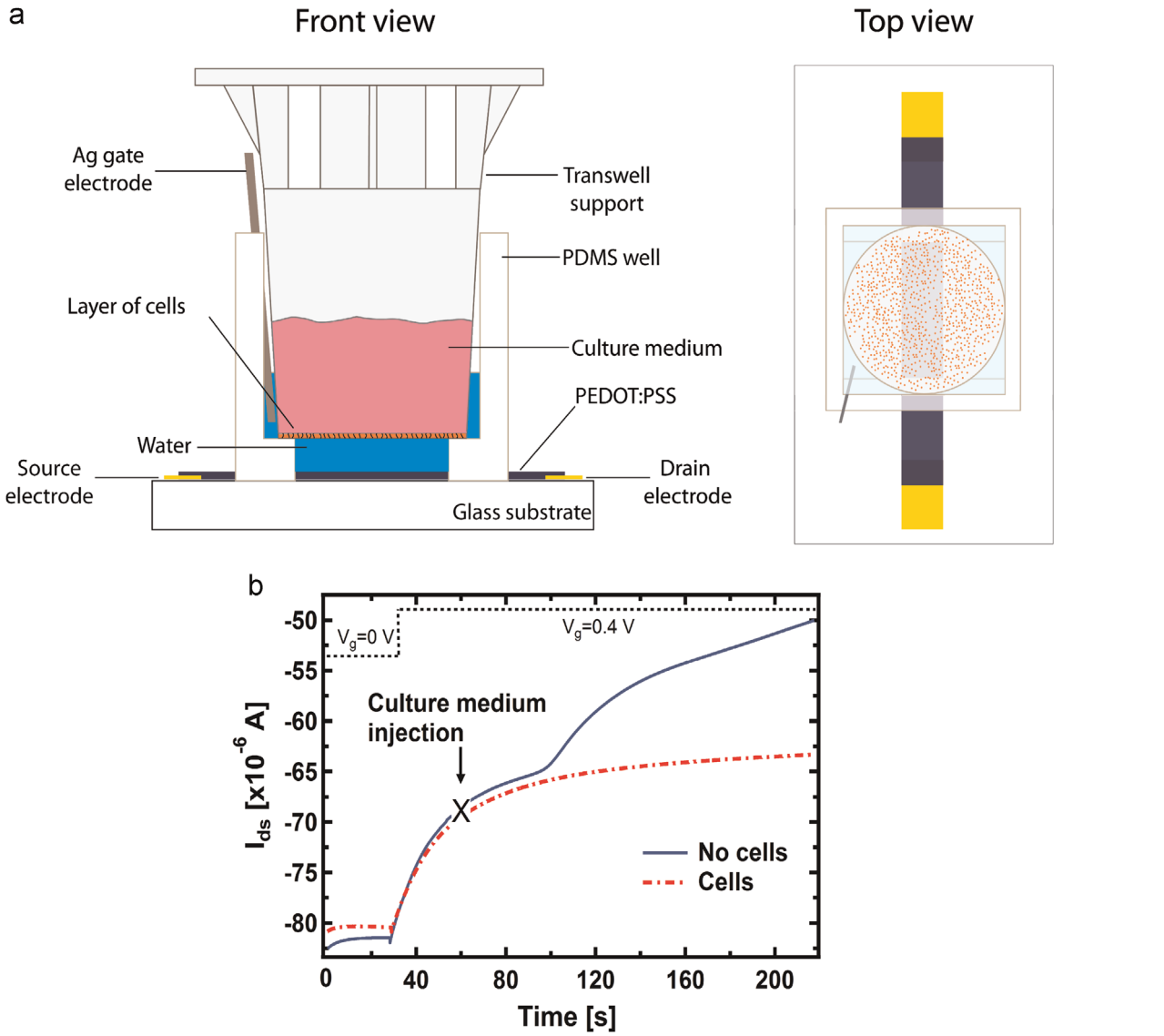

Fig. 1. (a) Experimental setup with the Twell support integrated in the OECT device. (b) Plot of the OECT I_{ds} current vs. time (transient current measurement). The dashed and continuous curves represent the measurement with and without cells cultured on the Twell membrane, respectively. The region above ~100 s represents the working range of the device where our biological sensing takes place.

performance typically induced by chemical processes when in direct contact with culture media or cells. A549 cancer cells were cultured on the Twell membrane prior to incorporation into the OECT. This cell line was chosen because it represents a common tumor epithelial cell-line *not forming* tight junctions and with a good sensitivity to doxorubicin (Litwiniec et al., 2010). The monolayer of cells grown on the Twell membrane shields the drift of cations from the culture medium through the membrane pores.

We first studied the working principle of our device, in order to model it and define its operational current range. We expected that the increase in ion density in the water layer should depend on the available free area of the Twell membrane. Hence, as a first step, we monitored the passage of cations from the electrolyte across the bare Twell membrane. Fig. 1b shows the plot of the measured current I_{ds} vs. time. The inner part of the Twell was initially left empty, while the OECT was electrically biased using the following parameters: $V_{ds}=-0.4$ V (set constant throughout all the measurement), $V_{gs}=0$ V ($t<30$ s) and $+0.4$ V ($t>30$ s). 150 μL RPMI culture medium were injected into the Twell 30 s after the gate voltage was turned on (that is, at $t=60$ s). The continuous curve in Fig. 1b highlights the evidence of the RPMI cations crossing the Twell membrane. The resulting signal, consisting of the decrease of $|I_{ds}|$, observed with a delay of ~40 s from the culture medium injection, represents the typical drift time of the cations coming from the culture medium across the membrane pores into the underlying water. Once crossed the porous membrane, as expected, the gate voltage V_{gs} forces them to enter the PEDOT:PSS channel, decreasing its conductivity. The dashed curve in Fig. 1b shows the pore screening effect due to cell growth. For a Twell where cells were grown for 48 h, the current signal of the OECT did not show any effect ascribable to ions drifting from the culture medium towards the underlying water. In fact, the shape of this curve is practically identical to that of an empty device, that is when the Twell is not filled with culture medium and no cells are cultivated on the membrane. From these results, we identify the region above ~100 s as the working range of the device, that is where our biological sensing takes place.

3.2. Modeling the device operation

In order to model the system it is important to observe that I_{ds} shows a linear dependence on time at the steady state ($t \geq 140$ s) for the bare Twell, instead of reaching the expected constant value. This behavior is correlated to the mechanism of cations drift from the electrolyte into the water layer. In our system the major driving force is, as in the case of the Fick's law (Bard and Faulkner, 2001), a concentration gradient. We therefore applied it to our specific case in the form

$$J = \frac{1}{G_0} G K_d \Delta C \tag{1}$$

where J is the net flux from the electrolyte through the Twell towards the water; G is the hydraulic conductance of the Twell expressed as $G=NG_{pore}$, where $N=n\Delta S_{Twell}$ is the total number of pores ($n=10^8/cm^2$ is the surface density of pores in the Twell membrane, as specified by the manufacturer, and $\Delta S_{Twell}=0.33$ cm^2 is the total surface of the Twell membrane) and G_{pore} is the conductance of a single pore of the Twell membrane; G_0 is the hydraulic conductance of the whole open Twell without membrane (in this case the Twell acts as an open vessel and Eq. (1) becomes the Fick's free diffusion in a vessel); K_d is the free diffusion coefficient of saline ions in liquids (typically $\sim 10^{-5}$ cm^2/s for diffusion of liquids with different concentrations); $\Delta C=C_1-C_2$ is the difference between the ionic concentrations of electrolyte (C_1) and water (C_2). On this basis, the correlation between the measured I_{ds} current and our experimental parameters can be finally expressed in the form (see Supplementary material for details)

$$I_{ds} \sim \gamma t \tag{2}$$

$$\gamma = \beta \frac{N r^4}{r_0^4} K_d \frac{N_\theta}{n} C_1 = dI_{ds}/dt \tag{3}$$

where $\beta=3.15\times10^{13}$ Am^{-1} mol^{-1} is a parameter that characterizes the Twell and is calculated from the previously mentioned linear slope of I_{ds} for the bare Twell (see Supplementary material); r is the radius of a single pore; r_0 is the radius of the whole micro-porous membrane; N_θ is the number of open pores available for diffusion across the Twell membrane ($N_\theta=N$ when no cells are seeded in the device); $n=10^8$/cm^2 is the surface density of pores in the Twell membrane, as specified by the manufacturer; and t is time. N_θ can be expressed as $N_\theta=N(1-\theta)$, where θ is the effective cell coverage of the membrane. Eq. (2) allows defining the device response, that is the angular coefficient γ of the linear region of I_{ds}. The direct dependence of γ on the number of open pores from Eq. (3) defines the sensing ability of the Twell-OECT, and allows evaluating the drug effect on the cells in terms of number of available open pores, which is the specific goal of the present work. The only approximation made is that the concentrations on both sides of the Twell membrane remain practically constant during the measurements, that is well confirmed in our conditions.

3.3. Viability assessment of doxorubicin-treated A549 cells

The evolution of cell death upon exposure to doxorubicin was studied by investigating both the time-dependence (cells exposed to 1 μM doxorubicin for 4, 8, and 24 h) and the concentration-dependence (cells exposed for 72 h to doxorubicin in the range from 0.5 to 10 μM). A549 cells were previously seeded in the Twells at a density of 10^5 cells/Twell and cultured for 48 h prior to electrical measurements. The seeding condition was chosen in order to reach a suitable cell density to effectively shield the diffusion of cations through the micro-porous membrane (see dashed curve in Fig. 1b). When exposed to doxorubicin, cells are expected to inherently change their morphology and biochemistry that, in turn, modifies cell–cell and cell–substrate interactions, therefore reducing the coverage of the Twell membrane pores. Consequently, the flux of ionic species across the Twell membrane increases, populating the water underneath and finally being detected by the OECT. Control experiments confirmed that pure doxorubicin at any concentration used here is not detected by our device. Noteworthy, due to our measurement procedure, the device never comes in contact with doxorubicin.

As reference, the cell death assessment was performed by means of a standard assay based on staining cells with fluorescent dyes, that specifically stain cells according to their viability status. This test gives the effect of doxorubicin on cell viability and the timescale through which the drug induces cell death. In our case it also represents a complementary standard biological technique for validating the OECT electrical signal. In more details, cell death was assessed by morphological studies performed using bright field- and fluorescence-microscopy on cells stained with Hoechst33342 and Propidium Iodide (PI). Hoechst provides a blue color both to healthy and early-stage apoptotic cells with non-damaged cell membrane, whereas PI stains with a red color the nucleus of necrotic and late apoptotic cells, where the integrity of the outer membrane has been damaged. An alternative cell viability test, the MTT (3-(4,5-dimethylthiazol-2yl)-2,5-diphenyltetrazolium bromide) assay, based on the conversion of MTT into

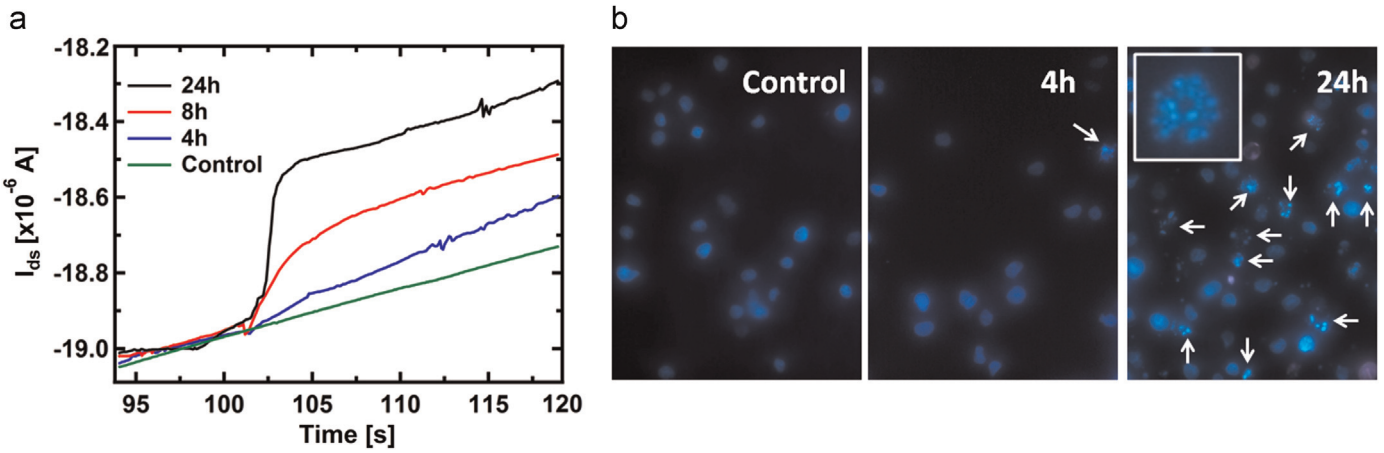

Fig. 2. (a) Kinetics of I_{ds} current as a function of different exposure times to 1 μM doxorubicin. (b) Representative pictures of the live/dead fluorescence assay of control cells and of cells exposed to 1 μM doxorubicin for 24 h. Cell death is prevalently due to apoptosis, as indicated by the white arrows. An exemplification of a single apoptotic cell is showed in the inset, where the typical fragmentation in apoptotic bodies can be observed.

formazan crystals by living cells with a constant mitochondrial activity, was also performed.

3.4. Electrical measurements on doxorubicin-treated A549 cells

3.4.1. Time-dependent effect of doxorubicin

First, the viability status of cells was monitored at three different times (4, 8, and 24 h) after the addition of a fixed dose (1 μM) of doxorubicin. Additional Twells, not exposed to doxorubicin, were used as control to exclude effects directly due to the cell growth conditions. After each exposure time, the Twells were integrated into the OECT, following a procedure similar to that described in the characterization and modeling of the device. Fig. 2a summarizes the typical experimental results. The change in I_{ds} is directly correlated to the drug exposure time of the cells as shown by the different response curves. As expected, no changes in the I_{ds} current were observed in the control sample (no exposure to doxorubicin) upon injection of the culture medium. We therefore have a first clear evidence that the drug producing stress and/or death on cells reduces the screening ability of cells on the ion drift towards the OECT. Furthermore, when compared to corresponding fluorescence images obtained by cell death assays (Fig. 2b) we obtain a further confirmation that the OECT measurements effectively correlate to the drug-induced cell death. In the presence of 1 μM doxorubicin the major morphological changes observed are characteristics of apoptosis (Fig. 2b) including cell shrinkage, cell membrane blebbing, chromatin condensation, and nucleosomal fragmentation (Fink and Cookson, 2005). The percentage of apoptotic cells increases in a time-dependent manner, from 5.5 ± 8.1% after 4 h to 25 ± 3% after 24 h exposure. Interestingly, the device was able to detect even alterations present at the earliest stage of apoptosis (4 h of treatment), which could possibly be ascribed to shape modification and volume shrinkage.

3.4.2. Dose-dependent effect of doxorubicin

In order to better qualify our Twell-OECT, we also studied the cell viability upon exposure to different concentrations of doxorubicin (0.5–10 μM) for 72 h. Cells were cultured in Twells and left to grow on the membrane for 48 h. Hence, controlled doses of doxorubicin were supplied and cells were left in incubation for 72 h. We therefore used the same previously described procedure to integrate the Twell into the OECT. Cell exposure to high doxorubicin doses and/or for a longer period of time induces cell death prevalently by necrosis, that is characterized by nuclear swelling with disruption of nuclear membrane structure, mitochondrial swelling, extensive cytoplasm vacuolization and cell lysis (Fink and Cookson, 2005). After 72 h of treatment at both low and high doses we were able to detect mainly necrotic and late apoptotic cells, and at this time cell death was expressed as percentage of PI-positive dead cells over the total number of counted cells, with a limiting value of 60% for drug concentrations higher than 5 μM (Fig. 3a). Fig. 3b shows the device dynamic response (I_{ds} vs. time) as a function of the drug concentration. We observed a clear differentiation of the I_{ds} time dependence with respect to the water benchmark as the drug concentration increases. The curves indicate that the number of ions crossing the micro-porous membrane is strongly increasing as the pores are cleared by the cells that die. We could detect effects induced by doxorubicin down to 0.5 μM without any optimization effort. However, our dynamic concentration range well covers the one commonly explored in cytotoxicity and pharmacological studies on cell cultures.

3.5. OECT response vs. standard biological assays

In order to achieve a final and quantitative calibration of our device we directly correlated the Twell-OECT response to the information obtained from the corresponding fluorescence images, giving the number of PI-positive dead cells as a function of the corresponding drug concentration (Fig. 3c). We used the device model described above for analyzing the Twell-OECT data. The fit of Eq. (2) to the I_d curves allows determining the number of open pores, as listed in Table S1 for the data of Fig. 3b. It is noteworthy that the device response and the fluorescence assay curves show very similar exponential behavior, with similar linear and saturating ranges. The major difference is observed in the slope at low drug concentrations, with a significantly higher response of the Twell-OECT. The observed behavior is likely related to the dynamics of cell death and to the stages of such processes to which the Twell-OECT is more sensitive. It is worth noting that at the lowest drug concentrations explored a significant amount of PI-negative early apoptotic cells may have been excluded from the count. To achieve a further insight into such question, we also compared the Twell-OECT information to the MTT viability test carried out on the same experiment. Fig. 3d demonstrates that the two measurements give the same trends over the whole range of drug concentrations, practically within the experimental uncertainties. This is another strong indication that the Twell-OECT is sensitive to a variety of processes inducing cell stress and death.

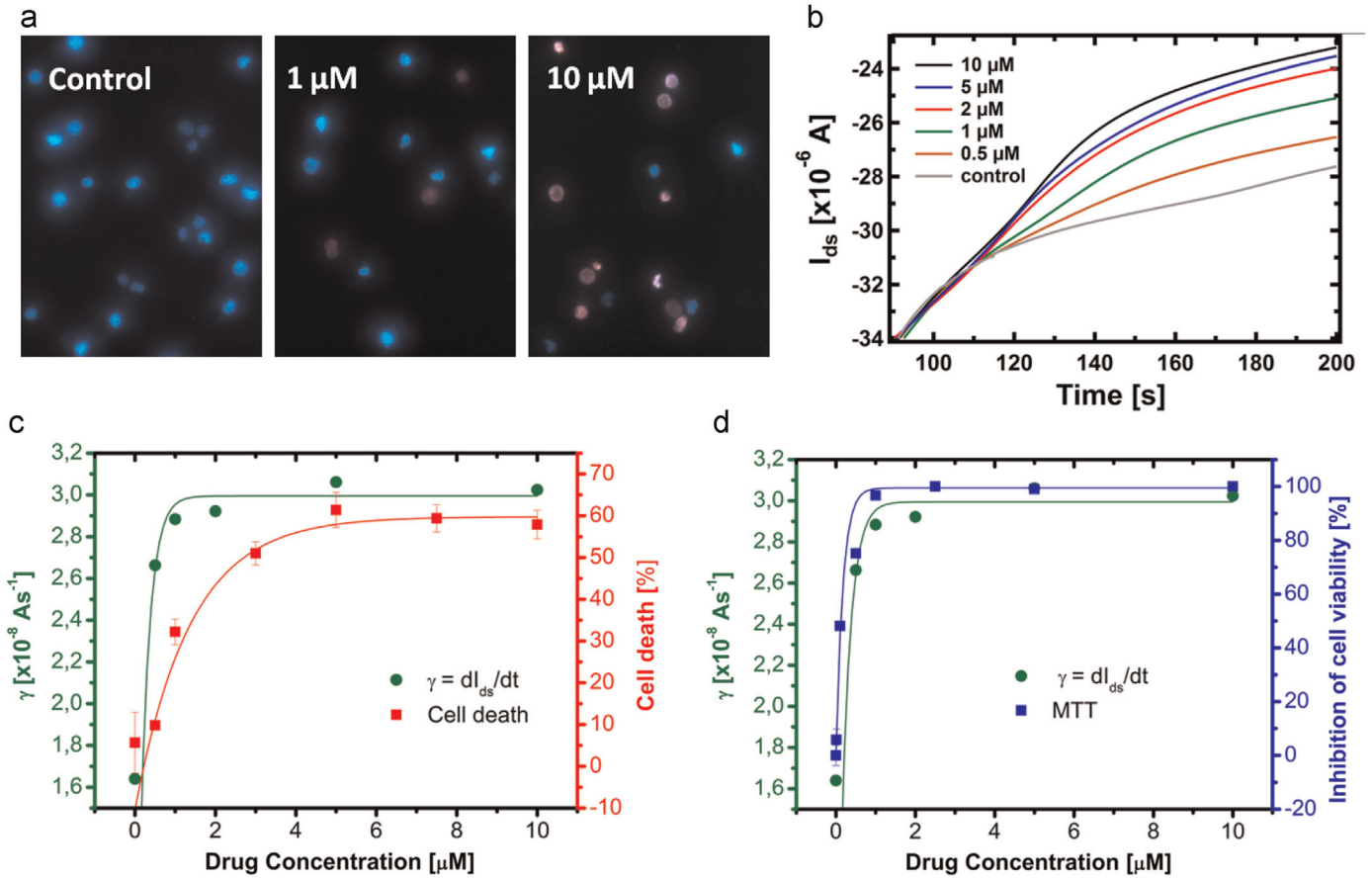

Fig. 3. (a) Representative pictures of the live/dead fluorescence assay upon 72 h exposure to increasing doses of doxorubicin. An increasing number of red cells (PI-positive) is observed as drug concentration increases. (b) Kinetics of I_{ds} current as a function of different concentrations of doxorubicin. (c) Direct comparison of the γ parameter (calculated with a linear fit from the linear region of I_{ds} vs. drug concentration) and data from the live/dead fluorescence assay, expressed as a function of drug concentration. (d) Direct comparison of the γ parameter and data from the MTT assay, as a function of drug concentration. Error bars in the γ curve and MTT data are much smaller than the markers size.

4. Conclusions

The Twell-OECT system proposed sensitively and reliably monitors cell death dynamics induced by exposure to drugs, detecting necrosis and early/late apoptosis. Our Twell-OECT shows responses comparable to state-of-the-art techniques, with the advantage of cost effectiveness, portability and ease of use, paving the way toward point-of-care diagnostics. Particularly relevant in our approach is the ability to follow real-time cellular dynamics avoiding cumbersome and expensive procedure and giving rise to novel opportunities for applications in toxicology, pharmacology, and therapeutics. In this framework, an important result is the observed high sensitivity to the early stages of cell deterioration mechanisms and to apoptotic events. We believe that our Twell-OECT can represent a system of choice in terms of performance and simplicity. From the proposed device model further developments are envisaged based on the optimization of the Twell-OECT system for different types of cells and cellular processes, extending its specific sensitivity to better discriminate the different death mechanisms.

Acknowledgements

This work has been supported by the project BioNiMed (Multifunctional Hybrid Nanosystems for Biomedical Applications) funded by the private bank fundation Fondazione Cassa di Risparmio di Parma (CARIPARMA) and by the N-Chem project within the CNR–NANOMAX Flagship program. Authors also acknowledge C. Fumarola for assistance on fluorescent assays and R. Mosca for fruitful discussions on electrical measurements.

Appendix A. Supplementary materials

Supplementary data associated with this article can be found in the online version at http://dx.doi.org/10.1016/j.bios.2015.01.073.

References

Bard, A.J., Faulkner, L.R., 2001. Electrochemical Methods: Fundamentals and Applications, 2nd Edition John Wiley & Sons, Inc., New York.
Berggren, M., Richter-Dahlfors, A., 2007. Organic bioelectronics. Adv. Mater. 19, 3201–3213.
Bernards, D., Malliaras, G.G., 2007. Steady-state and transient behavior of organic electrochemical transistors. Adv. Funct. Mater. 17, 3538–3544.
Bolin, M.H., Svennersten, K., Nilsson, D., Sawatdee, A., Jager, E.W.H., Richter-Dahlfors, A., Berggren, M., 2009. Active control of epithelial cell-density gradients grown along the channel of an organic electrochemical transistor. Adv. Mater. 21, 4379–4382.
Carterson, A.J., Höner zu Bentrup, K., Ott, C.M., Clarke, M.S., Pierson, D.L., Vanderburg, C.R., Buchanan, K.L., Nickerson, C.A., Schurr, M.J., 2005. A549 lung epithelial cells grown as three-dimensional aggregates : alternative tissue culture model for *Pseudomonas aeruginosa* pathogenesis. Infect. Immun. 73, 1129–1140.
Cavazzoni, A., Alfieri, R.R., Carmi, C., Zuliani, V., Galetti, M., Fumarola, C., Frazzi, R., Bonelli, M., Bordi, F., Lodola, A., Mor, M., Petronini, P.G., 2008. Dual mechanisms of action of the 5-benzylidene-hydantoin UPR1024 on lung cancer cell lines. Mol. Cancer Ther. 7, 361–370.
Cicoira, F., Santato, C. (Eds.), 2013. Organic Electronics: Emerging Concepts and

Technologies. WILEY-VCH Verlag GmbH, Weinheim, Ge.
DeFranco, J.A., Schmidt, B.S., Lipson, M., Malliaras, G.G., 2006. Photolithographic patterning of organic electronic materials. Org. Electron. 7, 22–28.
Fink, S.L., Cookson, B.T., 2005. MINIREVIEW apoptosis, pyroptosis, and necrosis: mechanistic description of dead and dying eukaryotic cells. Infect. Immun. 73, 1907–1916.
Gumus, A., Califano, J.P., Wan, A.M.D., Huynh, J., Reinhart-King, C. a, Malliaras, G.G., 2010. Control of cell migration using a conducting polymer device. Soft Matter 6, 5138.
Heijink, I.H., Brandenburg, S.M., Noordhoek, J. a, Postma, D.S., Slebos, D.-J., van Oosterhout, a J.M., 2010. Characterisation of cell adhesion in airway epithelial cell types using electric cell–substrate impedance sensing. Eur. Respir. J. 35, 894–903.
Hotchkiss, R.S., Strasser, A., McDunn, J.E., Swanson, P.E., 2009. Cell Death. New England J. Med. 361, 1570–1583.
Iannotta, S., D'Angelo, P., Romeo, A., Tarabella, G., 2015. Scalable and Flexible Bioelectronics and its Applications to Medicine In: Noh, Y.-Y., Caironi, M. (Eds.), Large-Area and Flexible Electronics. Wiley-VCH, Weinheim, Germany, pp. 487–541.
Isaksson, J., Kjall, P., Nilsson, D., Robinson, N.D., Berggren, M., Richter-Dahlfors, A., 2007. Electronic control of Ca 2+signalling in neuronal cells using an organic electronic ion pump. Nat. Mater. 6, 673–679.
Jimison, L.H., Tria, S., Khodagholy, D., Gurfinkel, M., Lanzarini, E., Hama, A., Malliaras, G.G., Owens, R.M., 2012. Measurement of barrier tissue integrity with an organic electrochemical transistor. Adv. Mater. 24, 5919–5923.
Kergoat, L., Piro, B., Simon, D.T., Pham, M.-C., Noël, V., Berggren, M., 2014. Detection of glutamate and acetylcholine with organic electrochemical transistors based on conducting polymer/platinum nanoparticle composites. Adv. Mater., 1–7.
Khodagholy, D., Doublet, T., Quilichini, P., Gurfinkel, M., Leleux, P., Ghestem, A., Ismailova, E., Hervé, T., Sanaur, S., Bernard, C., Malliaras, G.G., 2013. In vivo recordings of brain activity using organic transistors. Nat. Commun. 4, 1575.
Kroemer, G., Galluzzi, L., Vandenabeele, P., Abrams, J., Alnemri, E., Baehrecke, E., Blagosklonny, M., El-Deiry, W., Golstein, P., Green, D., Hengartner, M., Knight, R., Kumar, S., Lipton, S., Malorni, W., Nuñez, G., Peter, M., Tschopp, J., Yuan, J., Piacentini, M., Zhivotovsky, B., Melino, G., 2009. Classification of cell death: recommendations of the Nomenclature Committee on Cell Death 2009. Cell Death Differ. 16, 3–11.
Lin, P., Luo, X., Hsing, I.-M., Yan, F., 2011. Organic electrochemical transistors integrated in flexible microfluidic systems and used for label-free DNA sensing. Adv. Mater. 23, 4035–4040.
Lin, P., Yan, F., Yu, J., Chan, H.L.W., Yang, M., 2010. The application of organic electrochemical transistors in cell-based biosensors. Adv. Mater. 22, 3655–3660.
Litwiniec, A., Grzanka, A., Helmin-Basa, A., Gackowska, L., Grzanka, D., 2010. Features of senescence and cell death induced by doxorubicin in A549 cells: organization and level of selected cytoskeletal proteins. J. Cancer Res. Clin. Oncol. 136, 717–736.
Ramuz, M., Hama, A., Huerta, M., Rivnay, J., Leleux, P., Owens, R.M., 2014. Combined optical and electronic sensing of epithelial cells using planar organic transistors. Adv. Mater. 26, 7083–7090.
Rivnay, J., Owens, R.M., Malliaras, G.G., 2014. The rise of organic bioelectronics. Chem. Mater. 26, 679–685.
Simon, D.T., Kurup, S., Larsson, K.C., Hori, R., Tybrandt, K., Goiny, M., Jager, E.W.H., Berggren, M., Canlon, B., Richter-Dahlfors, A., 2009. Organic electronics for precise delivery of neurotransmitters to modulate mammalian sensory function. Nat. Mater. 8, 742–746.
Stoddart, M.J. (Ed.), 2011. Mammalian Cell Viability-Methods and Protocols. Springer Protocols, Davos Platz, Switzerland.
Tarabella, G., Mahvash Mohammadi, F., Coppedè, N., Barbero, F., Iannotta, S., Santato, C., Cicoira, F., 2013a. New opportunities for organic electronics and bioelectronics: ions in action. Chem. Sci. 4, 1395.
Tarabella, G., Nanda, G., Villani, M., Coppedè, N., Mosca, R., Malliaras, G.G., Santato, C., Iannotta, S., Cicoira, F., 2012. Organic electrochemical transistors monitoring micelle formation. Chem. Sci. 3, 3432.
Tarabella, G., Pezzella, A., Romeo, A., D'Angelo, P., Coppedè, N., Calicchio, M., D'Ischia, M., Mosca, R., Iannotta, S., 2013b. Irreversible evolution of eumelanin redox states detected by an organic electrochemical transistor: en route to bioelectronics and biosensing. J.Mater. Chem. B 1, 3843.
Tarabella, G., Santato, C., Yang, S.Y., Iannotta, S., Malliaras, G.G., Cicoira, F., 2010. Effect of the gate electrode on the response of organic electrochemical transistors. Appl. Phys. Lett. 97, 123304.
Tria, S., Jimison, L., Hama, A., Bongo, M., Owens, R., 2013. Sensing of EGTA mediated barrier tissue disruption with an organic transistor. Biosensors 3, 44–57.
Tria, S., Ramuz, M., Huerta, M., Leleux, P., Rivnay, J., Jimison, L.H., Hama, A., Malliaras, G.G., Owens, R.M., 2014. Dynamic monitoring of salmonella typhimurium infection of polarized epithelia using organic transistors. Adv. Healthcare MatEr. 3, 1–8.
Tybrandt, K., Forchheimer, R., Berggren, M., 2012. Logic gates based on ion transistors. Nat. Commun. 3, 871.
Wan, A.M.D., Brooks, D.J., Gumus, A., Fischbach, C., Malliaras, G.G., 2009. Electrical control of cell density gradients on a conducting polymer surface. Chem. Commun., 5278–5280.
Yang, F., Teves, S.S., Kemp, C.J., Henikoff, S., 2014. Doxorubicin, DNA torsion, and chromatin dynamics. Biochim, Biophys. Acta 1845, 84–89.
Yao, C., Xie, C., Lin, P., Yan, F., Huang, P., Hsing, I.-M., 2013. Organic electrochemical transistor array for recording transepithelial ion transport of human airway epithelial cells. Adv. Mater. 25, 6575–6580.
Zhu, Z., Mabeck, J.T., Zhu, C., Cady, N.C., Batt, A., Malliaras, G.G., 2004. A simple poly (3,4-ethylene dioxythiophene)/poly(styrene sulfonic acid) transistor for glucose sensing at neutral pH. Chem. Commun., 1556–1557.